

Radiative Emission of Neutrino Pairs in Atoms and Light Sterile Neutrinos

D. N. Dinh^{a)}, S. T. Petcov^{b,c)} ¹

^{a)}*Institute of Physics, Vietnam Academy of Science and Technology,
10 Dao Tan, Hanoi, Vietnam.*

^{b)}*SISSA and INFN-Sezione di Trieste,
Via Bonomea 265, 34136 Trieste, Italy.*

^{c)}*Kavli IPMU, University of Tokyo (WPI), Tokyo, Japan.*

Abstract

The process of Radiative Emission of Neutrino Pair (RENP) in atoms is sensitive to the absolute neutrino mass scale, the type of spectrum neutrino masses obey and the nature - Dirac or Majorana - of massive neutrinos. We analyse the possibility to test the hypothesis of existence of neutrinos with masses at the eV scale coupled to the electron in the weak charged lepton current in an RENP experiment. The presence of eV scale neutrinos in the neutrino mixing is associated with the existence of sterile neutrinos which mix with the active flavour neutrinos. At present there are a number of hints for active-sterile neutrino oscillations driven by $\Delta m^2 \sim 1 \text{ eV}^2$. We perform a detailed analysis of the RENP phenomenology within the “3 + 1” scheme with one sterile neutrino.

1 Introduction

All compelling neutrino oscillation data can be described within the reference 3-flavour neutrino mixing scheme with 3 light neutrinos ν_j having masses m_j not exceeding approximately 1 eV, $m_j \lesssim 1 \text{ eV}$, $j = 1, 2, 3$ (see, e.g., [1]). These data allowed to determine the parameters which drive the observed solar, atmospheric, reactor and accelerator flavour neutrino oscillations - the three neutrino mixing angles of the standard parametrisation of the Pontecorvo, Maki, Nakagawa and Sakata (PMNS) neutrino mixing matrix, θ_{12} , θ_{23} and θ_{13} , and the two neutrino mass squared differences Δm_{21}^2 and Δm_{31}^2 (or Δm_{32}^2) - with a relatively high precision [2, 3].

Although the mixing of the 3 flavour neutrino states has been experimentally well established, implying the existence of 3 light neutrinos ν_j having masses $m_j \lesssim 1 \text{ eV}$, there have been possible hints for the presence in the mixing of one or more additional neutrino states with masses at the eV scale. If these states exist, they must be related to the existence of one or more sterile neutrinos (sterile neutrino fields) which mix with the active flavour neutrinos (active flavour neutrino fields). The hints in question have been obtained: i) in the LSND $\bar{\nu}_\mu \rightarrow \bar{\nu}_e$ appearance experiment [4], in which a significant excess of events over the background is claimed to have been observed, ii) from the analysis of the $\bar{\nu}_\mu \rightarrow \bar{\nu}_e$ and $\nu_\mu \rightarrow \nu_e$ appearance data of the MiniBooNE experiment [5, 6], iii) from the re-analyses of

¹Also at: Institute of Nuclear Research and Nuclear Energy, Bulgarian Academy of Sciences, 1784 Sofia, Bulgaria

the short baseline (SBL) reactor neutrino oscillation data using newly calculated fluxes of reactor $\bar{\nu}_e$ [7, 8], which show a possible “disappearance” of the reactor $\bar{\nu}_e$ (“reactor neutrino anomaly”), and iv) from the data of the radioactive source calibrations of the GALLEX [9] and SAGE [10] solar neutrino experiments. The evidences for sterile neutrinos from the different data are typically at the level of up to approximately 3σ , except in the case of the LSND collaboration which claims a much higher C.L.

Significant constraints on the parameters characterising the oscillations involving sterile neutrinos follow from the negative results of the searches for $\nu_\mu \rightarrow \nu_e$ and/or $\bar{\nu}_\mu \rightarrow \bar{\nu}_e$ oscillations in the KARMEN [11], NOMAD [12], ICARUS [13] and OPERA [14] experiments, and from the nonobservation of effects of oscillations into sterile neutrinos in the solar neutrino experiments and in the studies of ν_μ and/or $\bar{\nu}_\mu$ disappearance in the CDHSW [15], MINOS [16] and SuperKamiokande [17] experiments. Constraints on the number and masses of sterile neutrinos are provided also by cosmological data (see, e.g., [18, 19, 20]). However, the constraints obtained so far cannot rule out the possibility of existence of one or two light sterile neutrinos which mix with the active flavour neutrinos.

Two “minimal” phenomenological models (or schemes) with light sterile neutrinos are widely used in order to explain the reactor neutrino and Gallium anomalies, the LSND and MiniBooNE data as well as the results of the negative searches for active-sterile neutrino oscillations: the so-called “3+1” and “3+2” models, which contain respectively one and two sterile neutrinos (right-handed sterile neutrino fields). The latter are assumed to mix with the 3 active flavour neutrinos (left-handed flavour neutrino fields) (see, e.g., [21, 22]). Thus, the “3 + 1” and “3 + 2” models have altogether 4 and 5 light massive neutrinos ν_j , which in the minimal versions of these models are Majorana particles. The additional neutrinos ν_4 and ν_5 , should have masses m_4 and m_5 at the eV scale (see further). It follows from the data that if ν_4 or ν_5 exist, they couple to the electron and muon in the weak charged lepton current with couplings U_{ek} and $U_{\mu k}$, $k = 4, 5$, which are approximately $|U_{ek}| \sim 0.1$ and $|U_{\mu k}| \sim 0.1$.

The hypothesis of existence of light sterile neutrinos with eV scale masses and the indicated charged current couplings to the electron and muon will be tested in a number of experiments with reactor and accelerator neutrinos, and neutrinos from artificial sources (see, e.g., [23, 24] for a detailed list and discussion of the planned experiments).

In the present article we analyse the possibility to test the hypothesis of existence of light sterile neutrinos which mix with the three active flavour neutrinos, i.e., the existence of more than 3 light massive Majorana neutrinos coupled to the electron in the weak charged lepton current, by studying the process of radiative emission of neutrino pair (RENP) in atoms [25] (see also, e.g., [26, 27] and references quoted therein). The RENP is a process of collective de-excitation of atoms in a metastable level into emission mode of a single photon plus a neutrino pair. The process of RENP was shown to be sensitive to the absolute values of the masses of the emitted neutrinos, to the type of spectrum the neutrino masses obey and to the nature - Dirac or Majorana - of massive neutrinos [25, 27]. If more than three light neutrinos couple to the electron in the weak charged lepton current and the additional neutrinos beyond the three known have masses at the eV scale, they will be emitted in the RENP process. This will lead to new observable features in the spectrum of the photon, emitted together with the neutrino pair. In the present article we analyse these features, concentrating for simplicity on the 3 + 1 phenomenological model with one sterile neutrino.

2 One Sterile Neutrino: the 3 + 1 Model

We begin by recalling that in the case of 3-neutrino mixing, the sign of $\Delta m_{31(32)}^2$ cannot be determined from the existing data and the two possible signs of $\Delta m_{31(2)}^2$, as it is well known, correspond to two types of neutrino mass spectrum. In the widely used convention of numbering the neutrinos ν_j with definite mass in the two cases (see, e.g., [1]) we shall also employ, the two spectra read:

i) *spectrum with normal ordering (NO)*: $0 \leq m_1 < m_2 < m_3$, $\Delta m_{31(32)}^2 > 0$, $\Delta m_{21}^2 > 0$, $m_{2(3)} = (m_1^2 + \Delta m_{21(31)}^2)^{\frac{1}{2}}$;

ii) *spectrum with inverted ordering (IO)*: $0 \leq m_3 < m_1 < m_2$, $\Delta m_{32(31)}^2 < 0$, $\Delta m_{21}^2 > 0$, $m_2 = (m_3^2 + \Delta m_{23}^2)^{\frac{1}{2}}$, $m_1 = (m_3^2 + \Delta m_{23}^2 - \Delta m_{21}^2)^{\frac{1}{2}}$.

Depending on the value of the lightest neutrino mass, $\min(m_j)$, the neutrino mass spectrum can be:

a) *Normal Hierarchical (NH)*: $m_1 \ll m_2 < m_3$, $m_2 \cong (\Delta m_{21}^2)^{\frac{1}{2}} \cong 8.68 \times 10^{-3}$ eV, $m_3 \cong (\Delta m_{31}^2)^{\frac{1}{2}} \cong 4.97 \times 10^{-2}$ eV; or

b) *Inverted Hierarchical (IH)*: $m_3 \ll m_1 < m_2$, with $m_{1,2} \cong |\Delta m_{32}^2|^{\frac{1}{2}} \cong 4.97 \times 10^{-2}$ eV; or

c) *Quasi-Degenerate (QD)*: $m_1 \cong m_2 \cong m_3 \cong m_0$, $m_j^2 \gg |\Delta m_{31(32)}^2|$, $m_0 \gtrsim 0.10$ eV, $j = 1, 2, 3$.

We will be interested in the 3 + 1 model, i.e., in the possibility of existence of one extra sterile neutrino beyond the three flavour neutrinos. In this case there will be four massive Majorana neutrinos, $\nu_{1,2,3,4}$, with ν_4 being the heaviest neutrino, $m_{1,2,3} < m_4$. Thus, the largest neutrino mass squared difference in the case of the 3 + 1 model with NO (IO) 3-neutrino mass spectrum will be $\Delta m_{41}^2 > 0$ ($\Delta m_{43}^2 > 0$).

In the case of the 3 + 1 scheme with NO neutrino mass spectrum, $m_1 < m_2 < m_3 < m_4$, the masses $m_{2,3,4}$ can be expressed in terms of the lightest neutrino mass m_1 and the three neutrino mass squared differences $\Delta m_{21}^2 > 0$, $\Delta m_{31}^2 > 0$ and $\Delta m_{41}^2 > 0$ as follows:

$$m_2 = \sqrt{m_{min}^2 + \Delta m_{21}^2}, \quad m_3 = \sqrt{m_{min}^2 + \Delta m_{31}^2}, \quad m_4 = \sqrt{m_{min}^2 + \Delta m_{41}^2}, \quad m_{min} \equiv m_1. \quad (1)$$

If the 3-neutrino mass spectrum of the 3 + 1 scheme is of IO type, the lightest neutrino mass is $m_{min} = m_3$, i.e., we have $m_3 < m_1 < m_2 < m_4$, $\Delta m_{21}^2 > 0$, $\Delta m_{32}^2 < 0$ and $\Delta m_{43}^2 > 0$. The masses $m_{1,2,4}$ are given by:

$$m_1 = \sqrt{m_{min}^2 + |\Delta m_{32}^2| - \Delta m_{21}^2}, \quad m_2 = \sqrt{m_{min}^2 + |\Delta m_{32}^2|}, \quad m_4 = \sqrt{m_{min}^2 + \Delta m_{43}^2}. \quad (2)$$

The mass spectra of the 3 + 1 NO (NH) and IO (IH) models are shown schematically in Figs. 1 and 2, where the figures were taken from [28].

In the 3+1 model there are four light massive neutrinos and, correspondingly, the neutrino mixing matrix - the Pontecorvo, Maki, Nakagawa and Sakata (PMNS) matrix - is a 4×4 unitary matrix. We will use the parametrisation of the PMNS matrix adopted in [21]:

$$U = O_{24}O_{23}O_{14}V_{13}V_{12} \text{diag}(1, e^{i\alpha_{21}/2}, e^{i\alpha_{31}/2}, e^{i\alpha_{41}/2}), \quad (3)$$

where O_{ij} and V_{kl} describe real and complex rotations in $i - j$ and $k - l$ planes, respectively, and α_{21} , α_{31} and α_{41} are three CP violation (CPV) Majorana phases [29]. Each of the 4×4

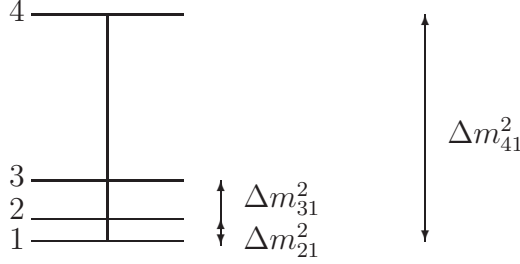


Figure 1: The Mass spectrum in the 3 + 1 NO (NH) model.

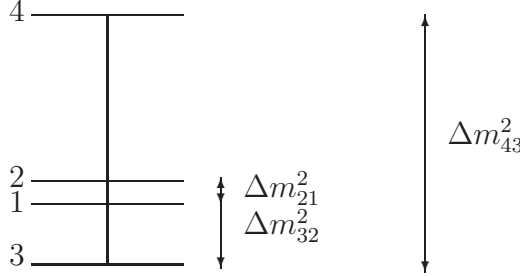


Figure 2: The mass spectrum in the 3+1 IO (IH) model.

matrices V_{12} and V_{13} contains one CPV phase, δ_{12} and δ_{13} , respectively, in their only two nonzero nondiagonal elements:

$$V_{ij} = D_{ij} O_{ij}(\theta_{ij}) D_{ij}^*, \quad (D_{ij})_{kr} = 0, \quad k \neq r, \quad (D_{ij})_{kk} = \begin{cases} e^{i\delta_{ij}}, & k = j; \\ 1 & k \neq j. \end{cases} \quad (4)$$

We did not include in U a possible additional matrix V_{34} corresponding to rotations in the 3-4 plane with angle θ_{34} (see, e.g., [21]), i.e., we have set $\theta_{34} = 0$, for simplicity. The angle θ_{34} , if nonzero, would be responsible for direct $\nu_\tau \rightarrow \nu_s$ oscillations. At present there do not exist data on this type of neutrino oscillations. We will comment later on the effects of $\theta_{34} \neq 0$ on the results of our analysis.

In this study we will use two reference sets of values of the three sterile neutrino oscillation parameters $\sin^2 \theta_{14}$, $\sin^2 \theta_{24}$ and Δm_{41}^2 (Δm_{43}^2)², which are obtained in the analyses performed in [21, 22]. We will use the best fit values

$$\sin^2 \theta_{14} = 0.0225, \quad \sin^2 \theta_{24} = 0.0296, \quad \Delta m_{41(43)}^2 = 0.93 \text{ eV}^2 \quad (\text{A}), \quad (5)$$

found in [21] in the global analysis of all the data (positive evidences and negative results) relevant for the tests of the sterile neutrino hypothesis. In ref. [21] a combined constraint on $\sin^2 \theta_{24}$ and $\sin^2 \theta_{34}$ was also obtained from the global analysis of the ν_μ disappearance data (see Fig. 5 (middle panel) in [21]). For the best fit value of $\sin^2 \theta_{24} = 0.0296$ and $\Delta m_{41(43)}^2 = 1.0 \text{ eV}^2$ this constraint implies $\sin^2 \theta_{34} \lesssim 0.05$ at 99% C.L. In what follows we will present results both for $\sin^2 \theta_{34} = 0$ and for $\sin^2 \theta_{34} = 0.05$.

²The neutrino mass squared difference Δm_{41}^2 (Δm_{43}^2) corresponds to NO (IO) 3-neutrino mass spectrum.

Global analysis of the sterile neutrino related data was performed, as we have already noticed, also in [22] (for earlier analyses see, e.g., [30]). The authors of [22] did not include in the data set used the MiniBooNE results at $E_\nu \leq 0.475$ GeV, which show an excess of events over the estimated background [31]. The nature of this excess is not well understood at present. For the best values of $\sin^2 \theta_{14}$ and $\Delta m_{41(43)}^2$ the authors of [22] find:

$$\sin^2 \theta_{14} = 0.0283, \quad \sin^2 \theta_{24} = 0.0124, \quad \Delta m_{41(43)}^2 = 1.60 \text{ eV}^2 \quad (\text{B}). \quad (6)$$

The quoted values of $\sin^2 \theta_{14}$ and $\Delta m_{41(43)}^2$ are close to the best fit values found in [21] in the analysis of the ν_e and $\bar{\nu}_e$ disappearance data: $\sin^2 \theta_{14} = 0.023$, $\Delta m_{41(43)}^2 = 1.78 \text{ eV}^2$. The authors of ref. [22] give also the allowed ranges of values of $\Delta m_{41(43)}^2$ and $\sin^2 \theta_{14,24}$ at various confidence levels. However, taking into account the uncertainties in the values of $\Delta m_{41(43)}^2$, $\sin^2 \theta_{14}$ and $\sin^2 \theta_{24}$ is beyond the scope of the present study.

In what concerns the 3-neutrino oscillations parameters $\sin^2 \theta_{12}$, $\sin^2 \theta_{23}$, $\sin^2 \theta_{13}$ and $\Delta m_{31(32)}^2$, in our numerical analysis we will use the their best fit values found in [2]:

$$\Delta m_{21}^2 = 7.54 \times 10^{-5} \text{ eV}^2, \quad |\Delta m_{31(32)}^2| = 2.47 \text{ (2.42)} \times 10^{-3} \text{ eV}^2, \quad (7)$$

$$\sin^2 \theta_{12} = 0.308, \quad \sin^2 \theta_{13} = 0.0234 \text{ (0.0240)}, \quad \sin^2 \theta_{23} = 0.437 \text{ (0.455)}, \quad (8)$$

where the values (the values in brackets) correspond to NO (IO) neutrino mass spectrum.

It should be added that global analyses of the neutrino oscillation data relevant for the test of the sterile neutrino hypothesis (positive evidences and the negative results) in the 3 + 1 scheme of interest, in which the 3-neutrino mixing parameters are treated as free parameters as well, have not been performed so far. Since the sterile neutrino mixing angles are of the order of 0.1 and they will affect the 3-neutrino mixing angles, in particular, via the unitarity conditions, $\sum_j |U_{lj}|^2 = 1$, $l = e, \mu$, one can expect naively that the changes, e.g., in $|U_{lj}|^2$, $j = 1, 2, 3$, where U_{lj} are the elements of the first and second rows of the neutrino mixing matrix, to be of the order of 0.01. Since $\sin^2 \theta_{13} = 0.0234$, one might expect, in particular, sizable effects on the value of $\sin^2 \theta_{13}$. However, the detailed study performed in ref. [21] showed that actually the value of $\sin^2 \theta_{13}$ as determined in 3 active neutrino oscillation analysis remains stable with respect to the presence of sterile neutrinos. The values of the other neutrino mixing parameters, relevant in our analysis, $\sin^2 \theta_{12} \cong 0.31 \gg 0.01$ and $\sin^2 \theta_{23} \cong 0.44 \text{ (0.45)} \gg 0.01$, and the effect of the presence of sterile neutrinos in the mixing is negligible for them.

Finally, in the analysis we will perform, the two Dirac and three Majorana CPV phases will be varied in their entire defining intervals.

3 The Process of RENP Involving Sterile Neutrinos

For a single atom, the process of radiative emission of neutrino pair (RENP) of interest is $|e\rangle \rightarrow |g\rangle + \gamma + (\nu_i + \nu_j)$, where ν_i 's are the neutrino mass eigenstates (see Fig. 3). In the case of interest we have $i, j = 1, 2, 3, 4$. If ν_i are Dirac fermions, $(\nu_i + \nu_j)$ should be understood as a pair of neutrino anti-neutrino with masses m_i and m_j , respectively. If neutrinos with definite mass are Majorana particles, we have $\bar{\nu}_i \equiv \nu_i$ and $(\nu_i + \nu_j)$ are the Majorana neutrinos with masses m_i and m_j . The proposed experimental method is to measure, under irradiation of

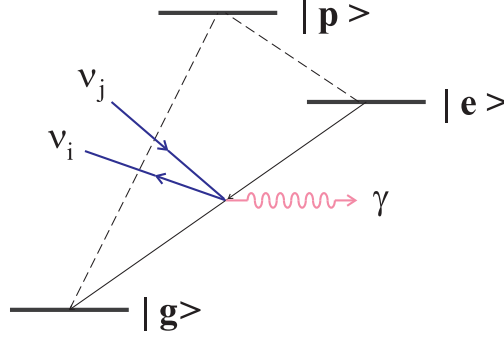


Figure 3: Atomic level scheme (of Λ -type [27]) for RENP $|e\rangle \rightarrow |g\rangle + \gamma + \nu_i \nu_j$, ν_i and ν_j being neutrino mass eigenstates.

two counter-propagating trigger lasers, the continuous photon (γ) energy spectrum below each of the thresholds ω_{ij} corresponding to the production of different pairs of neutrinos, $\nu_1 \nu_1, \nu_1 \nu_2, \nu_2 \nu_2, \dots$, $\omega < \omega_{ij}$, ω being the photon energy, and [25, 32]

$$\omega_{ij} = \omega_{ji} = \frac{\epsilon_{eg}}{2} - \frac{(m_i + m_j)^2}{2\epsilon_{eg}}, \quad i, j = 1, 2, \dots, \quad m_i, m_j \geq 0, \quad (9)$$

where ϵ_{eg} is the energy difference between the two relevant atomic levels. For four massive neutrinos there are altogether 10 different pairs $\nu_1 \nu_1, \nu_1 \nu_2, \dots, \nu_3 \nu_4, \nu_4 \nu_4$, and, correspondingly, 10 threshold energies ω_{ij} . The disadvantage of the method is the smallness of the RENP rate, which is proportional to G_F^2 , $G_F = 10^{-23} \text{eV}^{-2}$. This can possibly be overcome by “macro-coherence” amplification of the rate [33, 34], the amplification factor being $\propto n^2 V$, where n is the number density of excited atoms and V is the volume irradiated by the trigger laser. For n at the order of N_A / cm^3 , where N_A is Avogadro’s number, and $V \sim 100 \text{cm}^3$, the rate is observable. The macro-coherence of interest is developed by irradiation of two trigger lasers of frequencies ω_1, ω_2 , satisfying $\omega_1 + \omega_2 = \epsilon_{eg}$. It is a complicated dynamical process. The asymptotic state of fields and target atoms in the latest stage of trigger irradiation is described by a static solution of the master evolution equation. In many cases there is a remnant state consisting of field condensates (of the soliton type) accompanied with a large coherent medium polarisation. This asymptotic target state is stable against two photon emission (except for minor “leakage” from the edges of the target), while RENP occurs from any point in the target [33, 34]. A Group at Okayama University, Okayama, Japan, is working on the experimental realisation of the macro-coherent RENP [26].

As was indicated above, the physical observable of interest in the process of RENP, that, in principle, can be measured experimentally, is the single photon spectrum. The features of the photon spectrum in the case of 3-neutrino mixing, which allow to get information about the absolute neutrino mass scale, the neutrino mass spectrum and about the nature - Dirac or Majorana - of massive neutrinos, were discussed in detail on the example of a specific (combined $E1 \times M1$) atomic transition in [27]. Here we will generalise the results obtained in [27] to the case of the $3 + 1$ scheme with one sterile neutrino and four massive Majorana neutrinos. We will be primarily interested in the new photon spectrum features associated with the 4th massive Majorana neutrino related to the presence of the sterile neutrino in the

model. A detailed discussion of the atomic physics aspects of the problem is given, e.g., in [26].

The photon spectrum of interest, or more precisely, the photon spectral rate, i.e., the rate of number of events per unit time at each photon energy ω , in the cases of transitions in atoms considered in refs. [27] (see further), can be written as:

$$\Gamma_{\gamma 2\nu}(\omega) = \Gamma_0 I(\omega) \eta(t), \quad (10)$$

$$I(\omega) = \frac{1}{(\epsilon_{pg} - \omega)^2} \sum_{ij} |a_{ij}|^2 \Delta_{ij}(\omega) (I_{ij}(\omega) - \delta_M m_i m_j B_{ij}^M), \quad (11)$$

$$B_{ij}^M = \left(1 - 2 \frac{(\text{Im}(a_{ij}))^2}{|a_{ij}|^2} \right), \quad (12)$$

$$\Delta_{ij}(\omega) = \frac{1}{\epsilon_{eg}(\epsilon_{eg} - 2\omega)} \left\{ (\epsilon_{eg}(\epsilon_{eg} - 2\omega) - (m_i + m_j)^2) (\epsilon_{eg}(\epsilon_{eg} - 2\omega) - (m_i - m_j)^2) \right\}^{1/2}, \quad (13)$$

$$I_{ij}(\omega) = \left(\frac{1}{3} \epsilon_{eg}(\epsilon_{eg} - 2\omega) + \frac{1}{6} \omega^2 - \frac{1}{18} \omega^2 \Delta_{ij}^2(\omega) - \frac{1}{6} (m_i^2 + m_j^2) - \frac{1}{6} \frac{(\epsilon_{eg} - \omega)^2}{\epsilon_{eg}^2 (\epsilon_{eg} - 2\omega)^2} (m_i^2 - m_j^2)^2 \right), \quad (14)$$

Here Γ_0 determines the overall rate of the process and $\eta_\omega(t)$ is a dynamical dimensionless factor. Explicit expressions for both Γ_0 and $\eta_\omega(t)$ are given in [27]. Following the discussion in [27] (see also [32]), the factor $\eta_\omega(t)$ will be set to unity. Further, the factor $|a_{ij}|^2$ in the spectral function $I(\omega)$ is given in the case of the “3+1” scheme of interest by:

$$|a_{ij}|^2 = \left| U_{ei}^* U_{ej} - \frac{1}{2} \sum_{l=e,\mu,\tau} U_{li}^* U_{lj} \right|^2 = \left| U_{ei}^* U_{ej} - \frac{1}{2} (\delta_{ij} - U_{si}^* U_{sj}) \right|^2, \quad i, j = 1, \dots, 4, \quad (15)$$

where U_{si} and U_{sj} are two elements of the 4th row of the PMNS matrix. In the limit of $U_{si} = 0$, $i = 1, 2, 3, 4$, and for i, j taking values $i, j = 1, 2, 3$, the expression for $|a_{ij}|^2$, eq. (15), and for $I(\omega)$, eqs. (11) - (14), reduce to those corresponding to the reference scheme of mixing of 3 active flavour neutrinos with three light massive neutrinos. The term $\propto \delta_M m_i m_j B_{ij}^M$ in $I(\omega)$ appears only in the Majorana neutrino case: $\delta_M = 1$ ($\delta_M = 0$) if ν_j are Majorana (Dirac) particles. Let us add that, more generally, the term $\propto m_i m_j (1 - 2(\text{Im}(a_{ij}))^2/|a_{ij}|^2)$ is similar to, and has the same physical origin as, the term $\propto M_i M_j$ in the production cross section of two different Majorana neutralinos χ_i and χ_j with masses M_i and M_j in the process of $e^- + e^+ \rightarrow \chi_i + \chi_j$ [35]. The term $\propto M_i M_j$ of interest determines, in particular, the threshold behavior of the indicated cross section.

In the limit of massless neutrinos the spectral rate becomes

$$I(\omega; m_i = 0) = \frac{\omega^2 - 6\epsilon_{eg}\omega + 3\epsilon_{eg}^2}{12(\epsilon_{pg} - \omega)^2}, \quad (16)$$

where the prefactor of $\sum_{ij} |a_{ij}|^2 = 3/4$ is calculated using the unitarity of the neutrino mixing matrix.

In what follows we will perform a numerical analysis for the case of Yb atom and energy levels relevant for the RENP process of interest, for which a similar analysis was performed in the case of mixing of three active flavour neutrinos in [27]:

$$\text{Yb}; \quad |e\rangle = (6s6p)^3 P_0, \quad |g\rangle = (6s^2)^1 S_0, \quad |p\rangle = (6s6p)^3 P_1. \quad (17)$$

Table 1: The quantity $|a_{ij}| = |U_{ei}^* U_{ej} - \frac{1}{2} \sum_{l=e,\mu,\tau} U_{li}^* U_{lj}|$ (NO), case A

| $ a_{11} $ | $ a_{12} $ | $ a_{13} $ | $ a_{14} $ | $ a_{22} $ |
|-----------------|-----------------|-----------------|-----------------|-----------------|
| 0.1612 – 0.1822 | 0.4375 – 0.4471 | 0.1136 – 0.1350 | 0.0208 – 0.1047 | 0.1864 – 0.2058 |
| $ a_{23} $ | $ a_{24} $ | $ a_{33} $ | $ a_{34} $ | $ a_{44} $ |
| 0.0731 – 0.0941 | 0.0057 – 0.0989 | 0.4680 – 0.4731 | 0.0431 – 0.0664 | 0.0032 |

Table 2: The quantity $|a_{ij}| = |U_{ei}^* U_{ej} - \frac{1}{2} \sum_{l=e,\mu,\tau} U_{li}^* U_{lj}|$ (NO), case B

| $ a_{11} $ | $ a_{12} $ | $ a_{13} $ | $ a_{14} $ | $ a_{22} $ |
|-----------------|-----------------|-----------------|-----------------|-----------------|
| 0.1600 – 0.1753 | 0.4395 – 0.4465 | 0.1176 – 0.1308 | 0.0417 – 0.0963 | 0.1937 – 0.2076 |
| $ a_{23} $ | $ a_{24} $ | $ a_{33} $ | $ a_{34} $ | $ a_{44} $ |
| 0.0776 – 0.0891 | 0.0089 – 0.0831 | 0.4724 – 0.4761 | 0.0228 – 0.0485 | 0.0081 |

The atomic energy differences are [36]:

$$\epsilon_{eg} = 2.14349 \text{ eV}, \quad \epsilon_{pg} = 2.23072 \text{ eV}. \quad (18)$$

In the case of Yb atom considered, the overall rate factor Γ_0 is given by

$$\Gamma_0 \sim 0.37 \text{ mHz} \left(\frac{n}{10^{21} \text{ cm}^{-3}} \right)^3 \frac{V}{10^2 \text{ cm}^3}, \quad (19)$$

where the number is valid for the Yb first excited state of $J = 0$ ³.

In the present article we concentrate on the elementary particle physics potential of the proposed method to get information about the neutrino masses, neutrino mixing and the nature of massive neutrinos, and, more specifically, about the existence of more than three light massive neutrinos related to the existence of sterile neutrinos. The technical aspects of the possible experiment based on the method considered are discussed in, e.g., [26].

4 The Photon Spectrum Features in the Case of the “3 + 1” Scheme

It follows from eqs. (10) and (11) that the rate of emission of a given pair of neutrinos ($\nu_i + \nu_j$) is suppressed, in particular, by the factor $|a_{ij}|^2$, independently of the nature of massive neutrinos. In the case of mixing of 3 active flavour neutrinos and 3 massive neutrinos ν_j , $j = 1, 2, 3$, the 6 factors, corresponding to the emission of the 6 different neutrino pairs, $|a_{ij}|^2$, $i, j = 1, 2, 3$, do not depend on the CPV phases in the 3×3 unitary PMNS matrix; they depend only on the values of the angles θ_{12} and θ_{13} . The expressions for these 6 different factors $|a_{ij}|^2$, $i, j = 1, 2, 3$, in terms of the sines and cosines of the mixing angles θ_{12} and θ_{13} , are given in [27], where the values of $|a_{ij}|^2$ corresponding to the best fit values of $\sin^2 \theta_{12} = 0.307$ and $\sin^2 \theta_{13} = 0.0241$ (0.0244), obtained in the global analysis in [37], are also quoted (see Table 1 in [27]).

³ If one chooses the other intermediate path, 1P_1 , the rate Γ_0 is estimated to be of order, 1×10^{-3} mHz, a value much smaller than that of the 3P_1 path.

Table 3: The quantity $|a_{ij}| = |U_{ei}^* U_{ej} - \frac{1}{2} \sum_{l=e,\mu,\tau} U_{li}^* U_{lj}|$ (NO), case A, $\sin^2 \theta_{34} = 0.05$

| $ a_{11} $ | $ a_{12} $ | $ a_{13} $ | $ a_{14} $ | $ a_{22} $ |
|-----------------|-----------------|-----------------|-----------------|-----------------|
| 0.1631 – 0.1744 | 0.4425 – 0.4493 | 0.1019 – 0.1371 | 0.0431 – 0.0883 | 0.1987 – 0.2053 |
| $ a_{23} $ | $ a_{24} $ | $ a_{33} $ | $ a_{34} $ | $ a_{44} $ |
| 0.0667 – 0.0930 | 0.0239 – 0.0638 | 0.4329 – 0.4450 | 0.1185 – 0.1429 | 0.0269 |

In the case of the “3 + 1” scheme of interest with 4 massive neutrinos, there are altogether 10 factors $|a_{ij}|^2$, $i, j = 1, 2, 3, 4$, corresponding to the emission of the 10 different neutrino pairs. Moreover, in this case the factors of interest depend, in particular, on the Dirac and Majorana CPV phases present in the 4×4 unitary PMNS matrix⁴ given in eq. (3). By using the best fit values of the sterile neutrino mixing parameters in the cases A and B, quoted in eqs. (5) and (6), the 3-neutrino mixing parameters for NO neutrino mass spectrum given in eq. (8), and varying the Dirac and Majorana phases in the interval $[0, 2\pi]$, we have obtained the intervals of values in which the factors $|a_{km}|$, $k, m = 1, 2, 3, 4$, lie in the case of NO spectrum. The results are given in Tables 1 and 2. Performing a similar calculation assuming IO neutrino mass spectrum we found that the results for $|a_{km}|$, $k, m = 1, 2, 3, 4$, differ from those obtained for the NO spectrum by $\sim 10^{-3}$. Comparing the values of the factors $|a_{i,j}|$, $i, j = 1, 2, 3$, quoted in Table 1 in [27], with those given in Tables 1 and 2 we can conclude that the factors $|a_{i,j}|$ in the “3 + 1” scheme, which do not involve the 4th neutrino, i) change relatively little when one varies the two Dirac and the three Majorana CPV phases, and ii) can differ at most by approximately 0.02 from the factors in the 3-flavour neutrino mixing scheme. The same conclusion is valid in the case of IO neutrino mass spectrum. This implies that the presence of a 4th (sterile) neutrino in the mixing in the “3 + 1” scheme has a little effect on the sensitivities of the RENP process to the masses and the mixing of the three lighter neutrinos $\nu_{1,2,3}$, i.e., the absolute neutrino mass scale, the type of the neutrino mass spectrum and the nature of massive neutrinos, associated with the sub-mixing of the 3 active neutrinos, which were analysed in detail in [27]. This conclusion remains valid also for $\sin^2 \theta_{34} = 0.05$ in the case A of values of the sterile neutrino oscillation parameters. The factors $|a_{i,j}|$, $i, j = 1, 2, 3, 4$, in this case are given in Table 3. Comparing the values of $|a_{i,j}|$ in Tables 1 and 3 we see that a non-zero $\sin^2 \theta_{34} = 0.05$ leads to: i) a change of $|a_{i,j}|$, $i, j = 1, 2, 3$, by at most 0.01, except for the case $i = j = 3$, in which the change is approximately by 0.03; ii) a change in the minimal and maximal values of $|a_{14}|$ by 0.02, of $|a_{24}|$ - approximately by 0.02 and 0.035, and of the value of $|a_{44}|$ - approximately by 0.02. The largest is the change of the interval of values of $|a_{34}|$ - it is shifted to larger values by approximately 0.07.

Below we give a brief summary of the RENP phenomenology of the 3-flavour neutrino sub-mixing scheme, which practically coincides with the phenomenology and the results obtained in [27] by analysing the reference 3-flavour neutrino mixing scheme with three massive neutrinos.

⁴It follows from eqs. (3) and (15), in particular, that the quantities $|a_{ii}|$, $i = 1, 2, 3$, do not depend on the Majorana phases; they depend on the Dirac phases δ_{12} and δ_{13} only through the term $|U_{si}|^2$.

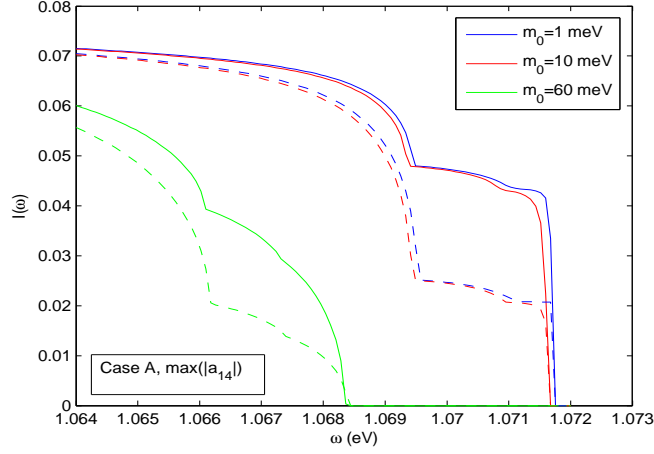


Figure 4: Photon energy spectra from the considered ${}^3P_0 \rightarrow {}^1S_0$ transition in Yb in the region of the 3-neutrino sub-mixing thresholds ω_{ij} , $i, j = 1, 2, 3$, in the “3 + 1” scheme with 4 massive Dirac neutrinos, for three sets of values of neutrino masses corresponding to $m_0 = 1, 10, 60\text{meV}$ and for NO (solid lines) and IO (dashed lines) neutrino mass spectrum. The spectra are obtained for the set A of values of neutrino oscillation parameters and for values of the CPV phases which maximise the factor $|a_{14}|$.

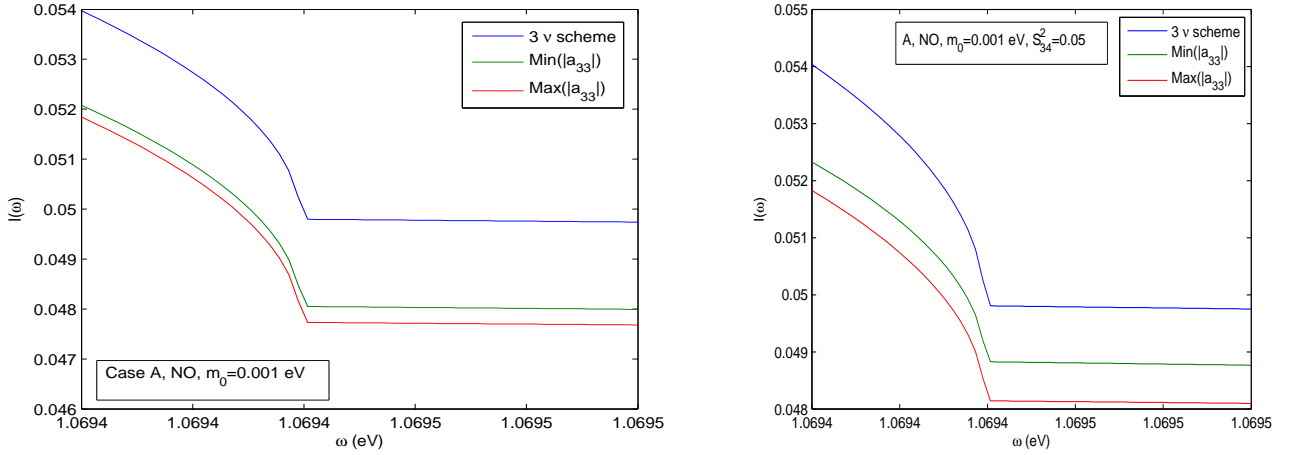


Figure 5: Photon energy spectrum from the ${}^3P_0 \rightarrow {}^1S_0$ transition in Yb in the region of the $(\nu_3 + \nu_3)$ emission threshold ω_{33} in the cases of 3-neutrino and “3+1”-neutrino mixing with massive Dirac neutrinos, for $m_0 = 1\text{ meV}$, and NO neutrino mass spectrum. In the case of “3+1”-neutrino mixing results in the case A for $\sin^2 \theta_{34} = 0$ (left panel) and 0.05 (right panel) and for the maximal and minimal values of $|a_{33}|$ are shown.

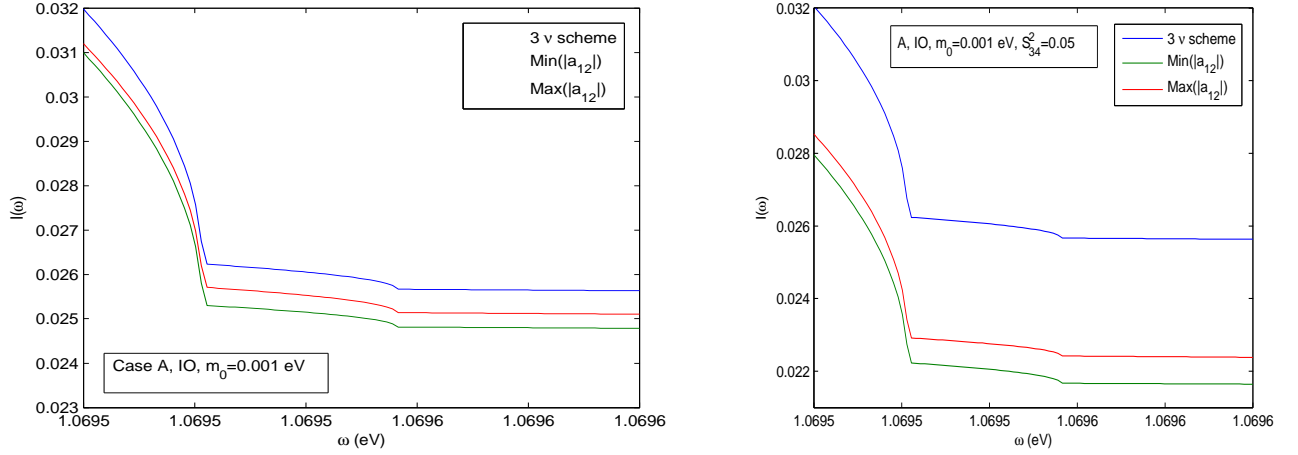


Figure 6: The same as in Fig. 5 but for IO neutrino mass spectrum and the $(\nu_1 + \nu_2)$ emission threshold. In the case of “3+1”-neutrino mixing results for the maximal and minimal values of $|a_{12}|$ are shown.

4.1 The 3-Flavour Neutrino Sub-Mixing: A Brief Summary of the RENP Phenomenology

All the neutrino physics information on the 3 light neutrino sub-mixing of interest is contained in the dimensionless spectral function $I(\omega)$ for values of ω near the thresholds ω_{ij} , $i, j = 1, 2, 3$. This is illustrated in Fig. 4 in which we show $I(\omega)$ for values of $\omega \leq \omega_{ij}$, $i, j = 1, 2, 3$, in the case of three massive Dirac neutrinos for three different sets of values of the neutrino masses (corresponding to the smallest mass $m_0 = 1, 10, 60$ meV) and for both the NO ($\Delta m_{31(32)}^2 > 0$) and IO ($\Delta m_{31(32)}^2 < 0$) neutrino mass spectra. We note that the locations of the thresholds corresponding to the three values of m_0 (and that can be seen in the figure) differ substantially. This feature can be used to determine the absolute neutrino mass scale, i.e., the smallest neutrino mass, as evident in differences of spectrum shapes for different masses of m_0 , 1, 10, 60 meV in Fig. 4. In particular, the smallest mass can be determined by locating the highest threshold (ω_{11} for NO and ω_{33} for IO). Also the location of the most prominent kink, which is due to the heavier neutrino pair emission thresholds (ω_{33} in the NO case and ω_{12} in the IO case), can independently be used to extract the smallest neutrino mass value. If the spectrum is of the NO type, the measurement of the position of the kink will determine the value of ω_{33} and therefore of m_3 . For the IO spectrum, the threshold ω_{12} is very close to the thresholds ω_{22} and ω_{11} . The rates of emission of the pairs $(\nu_2 + \nu_2)$ and $(\nu_1 + \nu_1)$, however, are smaller approximately by the factors 10.0 and 13, respectively, than the rate of emission of $(\nu_1 + \nu_2)$. Thus, the kink due to the $(\nu_1 + \nu_2)$ emission will be the easiest to observe. The position of the kink will allow to determine $(m_1 + m_2)^2$ and thus the absolute neutrino mass scale.

Once the absolute neutrino mass scale is determined, the distinction between the NO (NH) and IO (IH) spectra can be made by measuring the ratio of rates below and above the thresholds ω_{33} and ω_{12} (or ω_{11}), respectively. For $m_0 \lesssim 20$ meV and NH (IH) spectrum, for instance, the ratio of the rates at ω just above the ω_{33} (ω_{12}) threshold and sufficiently far

below the indicated thresholds, \tilde{R} , is $\tilde{R} \cong 0.70$ in the case of NH spectrum, and $\tilde{R} \cong 0.36$ if the spectrum is of the IH type (see also [27]). As Fig.4 indicates, this ratio changes little when m_0 increases up to $m_0 \cong 100$ meV.

The effect of the presence of the 4th neutrino ν_4 in the mixing on the photon spectrum in the region of the $\nu_3 + \nu_3$ ($\nu_1 + \nu_2$) emission threshold ω_{33} (ω_{12}) in the case of the “3+1” scheme, NO (IO) neutrino mass spectrum with $m_0 = 1$ meV, $\sin^2 \theta_{34} = 0$; 0.05 and Dirac neutrinos ν_j , is illustrated in Fig. 5 (Fig. 6). As Fig. 5 (Fig. 6) indicates, the presence of the 4th neutrino leads to an overall decreasing of the photon spectrum near the ω_{33} (ω_{12}) threshold by approximately 0.002 (0.001 - 0.003) in the NO (IO) case with respect to the spectrum corresponding to the 3-neutrino mixing. The quoted magnitude of the change of the spectrum remains practically the same when m_0 is increased up to 0.10 eV. In the case of IO spectrum it is maximal for $\sin^2 \theta_{34} = 0.05$. The observation of the indicated relatively small difference between the two photon spectra under discussion, corresponding the 3-neutrino and the (3+1)-neutrino mixing, requires a high precision measurement of the photon spectrum.

Determining the nature - Dirac or Majorana - of massive neutrinos by studying the process of RENP is very challenging experimentally. It is discussed in detail in [27] and we will consider it very briefly here for completeness. It is based on the fact that the rate of emission of a pair of Majorana neutrinos (particles) with masses m_i and m_j in the threshold region differs from the rate of emission (production) of a pair of Dirac neutrinos (particles) with the same masses by the presence of an interference term $\propto m_i m_j$ [35] in the emission (production) rate. In the case under discussion the interference term is proportional to $m_i m_j B_{ij}^M = m_i m_j (1 - 2(\text{Im}(a_{ij}))^2 / |a_{ij}|^2)$. In the discussion which follows we neglect the effects of the 4th neutrino which amounts to neglecting corrections $\sim 10^{-2}$. For $i = j$ we have $B_{ij}^M = 1$, the interference term is negative and tends to suppress the neutrino emission rate. In the case of $i \neq j$, the factor B_{ij}^M , and thus the rate of emission of a pair of different Majorana neutrinos, depends on specific combinations of the Majorana and Dirac CPV phases of the neutrino mixing matrix, which in the case of the reference 3-flavour neutrino mixing scheme were given for the first time in [27]. More specifically, neglecting corrections of the order of 10^{-2} , associated with the presence of the 4th neutrino ν_4 in the mixing⁵, we find:

$$B_{12}^M \cong \cos \alpha'_{21}, \quad B_{13}^M \cong \cos(\alpha_{31} - 2\delta_{13}), \quad B_{23}^M \cong \cos(\alpha'_{21} - \alpha_{31} + 2\delta_{13}), \quad \alpha'_{21} \equiv \alpha_{21} - 2\delta_{21}. \quad (20)$$

In contrast, the rate of emission of a pair of Dirac neutrinos in the case of 3-neutrino mixing does not depend on the CPV phases of the PMNS matrix. If CP invariance holds we have $\alpha_{21}, \alpha_{31} = 0, \pi$, $\delta_{21} = 0, \pi$, $\delta_{31} = 0, \pi$, and, correspondingly, $B_{ij}^M = -1$ or $+1$, $i \neq j = 1, 2, 3$. For $B_{ij}^M = +1$, the interference term tends to suppress the neutrino emission rate, while for $B_{ij}^M = -1$ it tends to increase it. If, e.g., α_{21} has a CP violating value we would have $-1 < B_{12}^M < +1$. Similar observation is valid for B_{13}^M and/or B_{23}^M provided, e.g., $\alpha_{31} \neq k\pi$ and/or $\alpha_{21} - \alpha_{31} \neq k'\pi$, $k, k' = 0, 1, 2$. Given the fact that, as it follows from Table 1 in [27] as well as from Tables 1 and 2, we have $|a_{12}|^2 \gg |a_{13}|^2, |a_{23}|^2$, the study of the emission of the neutrino pair $\nu_1 + \nu_2$ appears to be most promising for determination of the nature

⁵It is not difficult to show that the correction i) to B_{12}^M are of the order of $\max(s_{14}^2 c_{12} s_{12}, s_{14} s_{24} c_{12}^2, s_{24}^2 c_{12} s_{12})$, ii) to B_{13}^M are of the order of $\max(s_{14}^2 c_{12} s_{13}, s_{14} s_{24} c_{12} s_{23}, s_{24}^2 s_{12} s_{23})$, and iii) to B_{23}^M are of the order of $\max(s_{14}^2 s_{13} s_{12}, s_{14} s_{24} s_{12} s_{23}, s_{24}^2 c_{12} c_{23} s_{23})$.

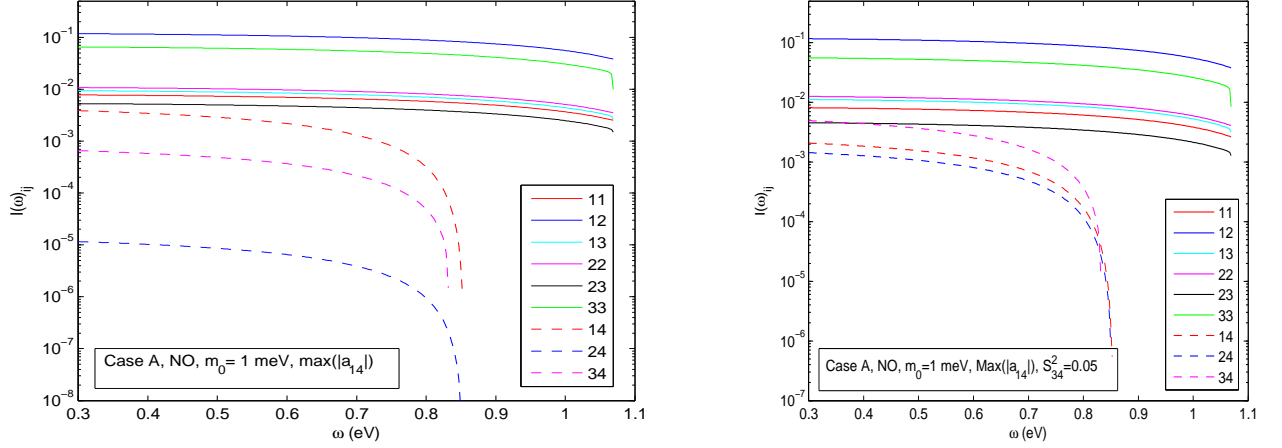


Figure 7: The photon spectra corresponding to the emission of the different individual neutrino pairs ($\nu_i + \nu_j$), $I_{ij}(\omega)$, in the case of the NO neutrino mass spectrum with $m_0 = 1$ meV and massive Dirac neutrinos. The spectra are obtained using the set A of values of the oscillation parameters, $\sin^2 \theta_{34} = 0$ (left panel) and 0.05 (right panel), and for the maximal value of $|a_{14}|$. The corresponding figures for IO neutrino mass spectrum look practically the same.

of massive neutrinos. In the case of NH spectrum, however, the term of interest $m_1 m_2 B_{12}^M$ can be strongly suppressed due to the relatively small value of m_1 . No such a suppression can take place for the IO spectrum, including the IH case. Further details regarding the problem of determination of the nature of the light massive neutrinos $\nu_{1,2,3}$ by measuring the spectrum of the photon emitted in the process of RENP can be found in [27].

4.2 The RENP Phenomenology of Emission of the 4th Neutrino with Mass at the eV Scale

It follows from Tables 1, 2 and 3 that, in what concerns the heaviest 4th neutrino ν_4 , for $\sin^2 \theta_{34} = 0$ (0.05) the largest maximal value $\sim (0.09 - 0.10)$ (~ 0.14) have the factors $|a_{14}|$ and $|a_{24}|$ (has the factor $|a_{34}|$), while the largest minimal value ~ 0.04 (~ 0.12) in the cases A and B have respectively the factors $|a_{34}|$ and $|a_{14}|$). Given the fact that the largest $|a_{ij}|$ factor is $|a_{12}| \sim (0.44 - 0.45)$ and corresponds to the emission of the $(\nu_1 + \nu_2)$ pair, the emission of the heaviest 4th neutrino ν_4 , even sufficiently far from the threshold, will proceed with rate which is for $\sin^2 \theta_{34} = 0$ (0.05) at least by a factor ~ 20 (~ 10) smaller than the rate of emission of the $(\nu_1 + \nu_2)$ pair. Near the threshold it will be further suppressed.

The predicted rate of emission of each of the individual pairs $(\nu_i + \nu_j)$, $I_{ij}(\omega)$, in the case of the NO spectrum with $m_0 = 1$ meV, for the set A of values of the neutrino oscillation parameters with $\sin^2 \theta_{34} = 0$ (left panel) and $\sin^2 \theta_{34} = 0.05$ (right panel) and maximal $|a_{14}|$, is shown in Fig. 7 as a function of the photon energy ω ⁶. Increasing m_0 up to $m_0 = 100$ meV leads to practically the same results for $I_{ij}(\omega)$ at ω sufficiently smaller than ω_{ij} . As

⁶We do not show the corresponding figures for IO neutrino mass spectrum because they are very similar to those shown for NO spectrum.

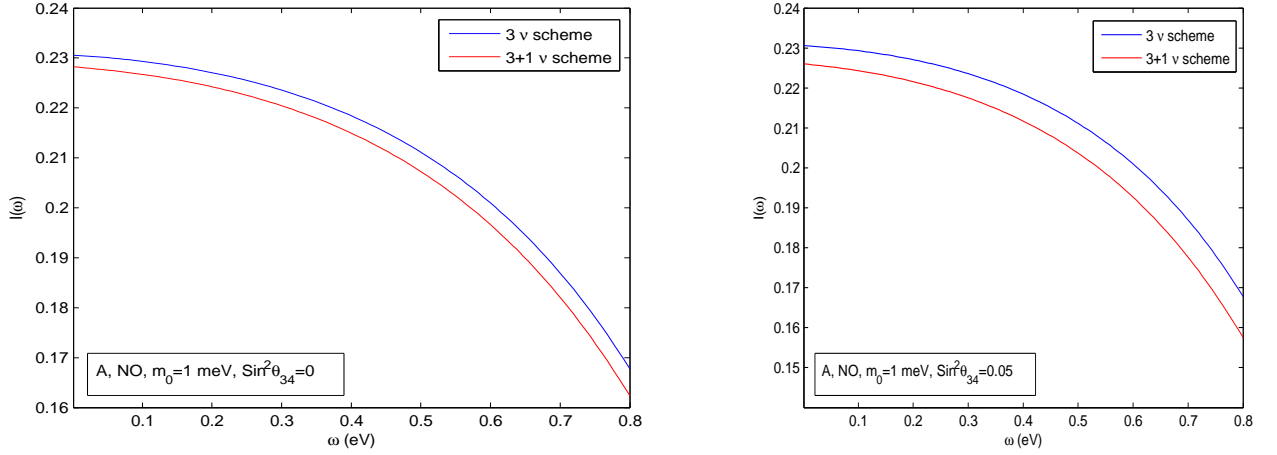


Figure 8: The spectral rates of 3-neutrino and (3 + 1)-neutrino schemes for the set A of neutrino oscillation data with $\sin^2 \theta_{34} = 0$ (left panel) and $\sin^2 \theta_{34} = 0.05$ (right panel).

Figs. 7 suggests and the preceding considerations imply, observing the contribution to the photon spectral rate due to the emission of pairs of neutrinos at least one of which is ν_4 would require a relatively high precision measurement of the photon spectrum at $\omega < \omega_{14}$. The same conclusion is valid for the set B of values of the neutrino oscillation parameters ($\sin^2 \theta_{34} = 0$). In Fig. 8 we present for NO neutrino mass spectrum the sum $I^{3\nu}(\omega) = \sum_{i,j=1,2,3} I_{ij}^{3\nu}(\omega)$, and the sum $I^{(3+1)} = \sum_{i,j=1,2,3,4} I_{ij}(\omega)$, as functions of ω in the region $\omega < \omega_{34}$, i.e., below the threshold of production of the neutrino pair $\nu_3 + \nu_4$ with the largest sum of masses⁷. The spectral rates $I_{ij}^{3\nu}(\omega)$, $i, j = 1, 2, 3$, have been computed assuming 3-neutrino mixing, i.e., no presence of sterile neutrinos in the mixing, while the rates $I_{ij}(\omega)$ have been calculated in the 3 + 1 scheme for the case A of sterile neutrino oscillation parameters and $\sin^2 \theta_{34} = 0$ and 0.05. As Fig. 8 shows, the total spectral rates $I^{3\nu}(\omega)$ and $I^{(3+1)}(\omega)$ differ by approximately (0.005 - 0.010) for ω sufficiently smaller than the threshold energy ω_{34} . This difference is independent of the value of $m_0 \leq 100$ meV. The same conclusion is valid in the case of the IO neutrino mass spectrum. The indicated difference can be used, in principle, to test the hypothesis of existence of a 4th (sterile) neutrino with a mass at the eV scale in a RENP type of experiment. Such a test would require a rather precise calculation of the total spectral rate $I^{3\nu}(\omega)$ at sufficiently small values of $\omega < \omega_{ij}$, $i, j = 1, 2, 3$. Given the fact that at the values of ω of interest $I^{3\nu}(\omega)$ is practically independent of the values of the neutrino masses, a calculation of $I^{3\nu}(\omega)$ with the requisite precision might not be impossible.

Further, the threshold energy ω_{14} for the emission of the $\nu_1 + \nu_4$ pair is well separated from the energy thresholds of the emission of pairs of the 3 light neutrinos ω_{ij} , $i, j = 1, 2, 3$. This is clearly seen also in Fig. 7. Indeed, for the NO (IO) spectrum with $m_0 = 0.001$; 0.01 eV, for instance, the thresholds ω_{ij} for $i, j = 1, 2, 3$ are grouped in the vicinity of 1.07 eV, while $\omega_{14} \cong 0.85$ eV ($\omega_{14} \cong 0.83$ eV). Similar results are valid for $m_0 = 0.10$ eV.

The threshold ω_{34} is relatively close to ω_{14} . Indeed, for, e.g., $m_0 = 0.001$ (0.100) eV

⁷In the case of the transitions between the atomic energy levels considered and the values of $\Delta m_{14(34)}^2$ used in our analysis, the pair $\nu_4 + \nu_4$ cannot be emitted in the process of interest.

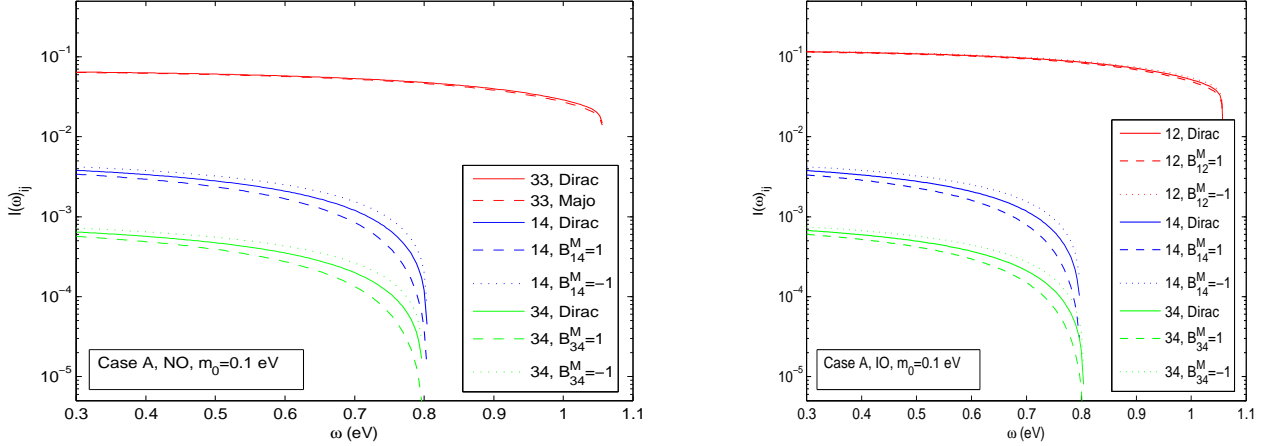


Figure 9: The photon spectra $I_{14}(\omega)$ and $I_{34}(\omega)$ in the case of i) Dirac neutrinos (solid lines), ii) Majorana neutrinos and $B_{14}^M, B_{34}^M = +1$ (dashed lines), and iii) Majorana neutrinos and $B_{14}^M, B_{34}^M = -1$ (dotted lines), in the case of the NO (left panel) and IO (right panel) neutrino mass spectra with $m_0 = 0.1$ eV. We show for comparison also the spectrum $I_{33}(\omega)$ ($I_{12}(\omega)$) in the left (right) panel. The spectra are obtained using the set A of values of the oscillation parameters and for $\delta_{12} = \delta_{13} = 0$ (i.e., for maximal $|a_{14}|$), $\alpha_{31} = 0$ and $\alpha_{21} = \pi$ (0.517) (left panel) and $\alpha_{21} = 0$ (π) (right panel), corresponding, respectively, to $B_{34}^M = +1$ (-1) and $B_{12}^M = +1$ (-1).

and NO neutrino mass spectrum we have $\omega_{14} = 0.8544$ (0.8049) and $\omega_{34} = 0.8319$ (0.7991). For IO spectrum and the same values of m_0 we get $\omega_{14} = 0.8325$ (0.7993) and $\omega_{34} = 0.8544$ (0.8049). Distinguishing between the threshold energies ω_{14} and ω_{34} would not be a problem, in principle, since it is expected that in the RENP experiments the photon energy will be known with a relative uncertainty of $\sim 10^{-5}$. It should be added, however, that for the values of $\delta_{12} = \delta_{13} = 0$, for which $|a_{14}|^2$ has a maximal value, and, e.g., for the set A of the neutrino oscillation parameters, $|a_{34}|^2$ is approximately by a factor of 6 smaller than $|a_{14}|^2$.

In the case of Majorana neutrinos, the factor B_{14}^M , associated with the emission of $\nu_1 + \nu_4$, is given by a somewhat lengthy expression. For $\delta_{12}, \delta_{13} = 0$ or π we have:

$$B_{14}^M = \cos \alpha_{41}. \quad (21)$$

In Fig. 9 we illustrate the effects of the term $\propto m_i m_j B_{ij}^M$ on the individual spectra $I_{14}(\omega)$ and $I_{34}(\omega)$ of emission of the pairs of Majorana neutrinos $\nu_1 + \nu_4$ and $\nu_3 + \nu_4$ in the cases of NO (left panel) and IO (right panel) neutrino mass spectra with $m_0 = 0.1$ eV. We show for comparison also the spectrum $I_{33}(\omega)$ ($I_{12}(\omega)$) in the left (right) panel at $\omega < \omega_{33}$ ($\omega < \omega_{12}$) outside the threshold region. The spectra are obtained using the set A of values of the oscillation parameters and for $\delta_{12} = \delta_{13} = 0$ (i.e., for maximal $|a_{14}|$), $\alpha_{31} = 0$ and $\alpha_{21} = \pi$ (0.517) (left panel) and $\alpha_{21} = 0$ (π) (right panel), corresponding, respectively, to $B_{34}^M = +1$ (-1) and $B_{12}^M = +1$ (-1). As Fig. 9 indicates, the effect of the terms $\propto m_i m_j B_{ij}^M$ on the spectra $I_{14}(\omega)$ and $I_{34}(\omega)$ can be sizable in the threshold region. In the case of NO spectrum, the term $\propto m_1 m_4 B_{14}^M$ can be suppressed due to a small value of the

Table 4: The quantity $|a_{ij}| = |U_{ei}^* U_{ej} - \frac{1}{2} \sum_{l=e,\mu,\tau} U_{li}^* U_{lj}|$ (NO), case B, $\sin^2 \theta_{14} = 0.058$, $\sin^2 \theta_{24} = 0.016$.

| $ a_{11} $ | $ a_{12} $ | $ a_{13} $ | $ a_{14} $ | $ a_{22} $ |
|-----------------|-----------------|-----------------|-----------------|-----------------|
| 0.1410 – 0.1679 | 0.4273 – 0.4396 | 0.1113 – 0.1328 | 0.0748 – 0.1354 | 0.1937 – 0.2181 |
| $ a_{23} $ | $ a_{24} $ | $ a_{33} $ | $ a_{34} $ | $ a_{44} $ |
| 0.0733 – 0.0912 | 0.0289 – 0.1113 | 0.4707 – 0.4773 | 0.0200 – 0.0591 | 0.0265 |

lightest neutrino mass m_1 . Such a suppression will not hold for IO spectrum. However, the observation of the effects of the terms $\propto m_1 m_4 B_{14}^M$ and/or $\propto m_3 m_4 B_{34}^M$ on the total photon spectrum $I(\omega)$ in the case of massive Majorana neutrinos is very challenging due to the relatively small values of the factors $|a_{14}|^2$ and $|a_{34}|^2$. Such small values are a consequence of the relatively small phenomenologically allowed couplings of the 4th (sterile) neutrino ν_4 to the electron in the weak charged lepton current.

The results described in the present Section have been obtained for the best fit values of the sterile neutrino oscillation parameters quoted in eqs. (5) and (6). In ref. [22] the 3σ allowed ranges of the parameters of interest were also reported. For $\Delta m_{41(43)}^2$ this range reads: $0.82 \text{ eV}^2 \lesssim \Delta m_{41(43)}^2 \lesssim 2.19 \text{ eV}^2$. The 3σ maximal values of $\sin^2 \theta_{14}$ and $\sin^2 \theta_{24}$ found in [22] are the following: $\sin^2 \theta_{14} \lesssim 0.058$ and $\sin^2 \theta_{24} \lesssim 0.016$. For $\sin^2 \theta_{14} = 0.058$ and $\sin^2 \theta_{24} = 0.016$, the values of the factors $|a_{ij}|$ are given in Table 3. Comparing them with the values quoted in Tables 1 and 2 we see that the RENP rate for emission of the pair of neutrinos ($\nu_1 + \nu_4$) can be approximately by a factor 1.8 larger than the rate predicted using the best fit values of $\sin^2 \theta_{14}$ and $\sin^2 \theta_{24}$ quoted in eqs. (5) and (6). The rates of emission of the neutrino pairs ($\nu_2 + \nu_4$) and ($\nu_3 + \nu_4$) can also be larger, but by smaller factors. In the case of the atomic levels considered the emission of the pair ($\nu_4 + \nu_4$) cannot take place because the energy of the transition available for the emission of the neutrinos is smaller than $2m_4$.

5 Summary and Conclusions

We have analysed the possibility to test the hypothesis of existence of neutrinos with masses at the eV scale coupled to the electron in the weak charged lepton current in an atomic physics experiment on radiative emission of neutrino pair (RENP), in which the spectrum of the photon is measured with high precision. The RENP is a process of collective de-excitation of atoms in a metastable level into emission mode of a single photon plus a neutrino pair [25]. The process of RENP was shown to be sensitive to the absolute values of the masses of the emitted neutrinos, to the type of spectrum the neutrino masses obey and to the nature - Dirac or Majorana - of massive neutrinos [25, 27]. If more than three light neutrinos couple to the electron in the weak charged lepton current and the additional neutrinos beyond the three known have masses at the eV scale, they will be emitted in the RENP process. This will lead to new observable features in the spectrum of the photon, emitted together with the neutrino pair. The presence of eV scale neutrinos in the neutrino mixing is associated with the existence of sterile neutrinos which mix with the active flavour neutrinos. At present there are a number of hints for active-sterile neutrino oscillations driven by $\Delta m^2 \sim 1 \text{ eV}^2$. In the present article we have investigated these features, concentrating for simplicity on the

3 + 1 phenomenological model with one sterile neutrino. We have used two sets of values of the three additional neutrino mixing parameters of the 3 + 1 model relevant for our study - $\sin^2 \theta_{14}$, $\sin^2 \theta_{24}$ and $\Delta m_{41(43)}^2$ - given in eqs. (5) and (6). These values were found in the global analyses of all the data (positive evidences and negative results) relevant for the tests of the sterile neutrino hypothesis, performed in [21] and [22], respectively.

The emission of the neutrino pair ($\nu_i + \nu_j$) will lead to a kink in the photon spectrum at the threshold energy $\omega_{ij} = \omega_{ji}$. For three massive neutrinos of the “standard” 3-neutrino mixing scheme there are altogether 6 different pairs $\nu_1 + \nu_1$, $\nu_1 + \nu_2, \dots, \nu_3 + \nu_3$, and, correspondingly, 6 threshold energies ω_{ij} . In the “3 + 1” model there are 4 additional pairs $\nu_1 + \nu_4$, $\nu_2 + \nu_4$, $\nu_3 + \nu_4$ and $\nu_4 + \nu_4$, and therefore altogether 10 thresholds. The magnitude of the contribution of the ($\nu_i + \nu_j$) emission to the photon spectral rate is determined essentially by the factor $|a_{ij}|^2$ (eq. (15)), which depends only on the neutrino mixing angles and the CP violation phases present in the neutrino mixing matrix. For the two sets of the sterile neutrino oscillation parameters considered by us the possible values of the factors $|a_{ij}|$ are given in Tables 1 and 2.

We have shown, in particular, that the presence of the 4th neutrino of the “3+1” scheme leads to an overall decreasing of the photon spectral rate near the prominent 3-neutrino mixing threshold ω_{33} (ω_{12}) by approximately 0.002 (0.001) with respect to the rate corresponding to the 3-neutrino mixing. The quoted magnitude of the change of the spectral rate remains practically the same for values of the lightest neutrino mass $m_0 \lesssim 0.10$ eV. The observation of the indicated relatively small difference between the two photon spectral rates under discussion, corresponding the 3-neutrino and the (3+1)-neutrino mixing, requires a high precision measurement of the photon spectrum. The quoted result illustrates the more general conclusion reached in the present study, namely, that the presence of a 4th (sterile) neutrino in the mixing in the “3 + 1” scheme has a little effect on the sensitivities of the RENP process to the masses and the mixing of the three lighter neutrinos $\nu_{1,2,3}$, i.e., the absolute neutrino mass scale, the type of the neutrino mass spectrum and the nature of massive neutrinos, associated with the sub-mixing of the 3 active neutrinos.

The threshold energy ω_{14} for the emission of the $\nu_1 + \nu_4$ ($\nu_3 + \nu_4$) pair which in the cases A with $\sin^2 \theta_{34} = 0$ ($\sin^2 \theta_{34} = 0.05$) has the largest $|a_{ij}|$ factor for $i = 1, 2, 3, 4$ and $j = 4$ (i.e., for emission of a pair of neutrinos at least one of which is the heaviest neutrino ν_4), was shown to be well separated from the energy thresholds of the emission of pairs of the 3 light neutrinos ω_{ij} , $i, j = 1, 2, 3$. As the numerical analysis performed by us allowed to conclude, the emission of the heaviest 4th neutrino ν_4 , even sufficiently far from the threshold, is predicted to proceed with rate which is at least by a factor ~ 20 (~ 10) smaller than the rate of emission of the lighter ($\nu_1 + \nu_2$) pair having the largest $|a_{ij}|$ factor. Near the threshold it will be further suppressed. At values of the photon energy ω , which are sufficiently smaller than $\min(\omega_{ij})$, $i, j = 1, 2, 3, 4$, the total spectral rate in the case of mixing of 3 neutrinos only, i.e., no presence of sterile neutrino(s) in the mixing, $I^{3\nu}(\omega) = \sum_{i,j=1,2,3} I_{ij}^{3\nu}(\omega)$, and the total spectral rate in the 3 + 1 scheme, $I^{(3+1)}(\omega) = \sum_{i,j=1,2,3,4} I_{ij}(\omega)$, differ approximately by 0.010. This difference can be used, in principle, to test the hypothesis of existence of a 4th (sterile) neutrino with a mass at the eV scale in a RENP type of experiment. Such a test would require a rather precise calculation of the the total spectral rate $I^{3\nu}(\omega)$ at sufficiently small values of $\omega < \omega_{ij}$, $i, j = 1, 2, 3$. At the values of ω of interest the 3-neutrino total spectral rate $I^{3\nu}(\omega)$ is practically independent of the neutrino masses and a calculation of $I^{3\nu}(\omega)$ with the requisite precision might not be impossible.

The results obtained in the present study show that observing in an RENP experiment the contribution to the photon spectral rate due to the emission of pairs of neutrinos at least one of which is the eV scale neutrino ν_4 of the “3+1” scheme with one sterile neutrino would be very challenging since it would require a relatively high precision measurement of the photon spectral rate.

Acknowledgments

This work was supported in part by the Vietnam National Foundation for Science and Technology Development (NAFOSTED) under the grant 103.03-2012.49 (D.N.D.), by the INFN program on “Theoretical Astroparticle Physics” (TASP), by the research grant 2012CPPYP7 (*Theoretical Astroparticle Physics*) under the program PRIN 2012 funded by the Italian Ministry of Education, University and Research (MIUR), by the World Premier International Research Center Initiative (WPI Initiative), MEXT, Japan, and by the European Union FP7-ITN INVISIBLES and UNILHC (Marie Curie Action, PITAN-GA-2011-289442 and PITN-GA-2009-23792) (S.T.P.).

References

- [1] K. Nakamura and S. T. Petcov, in J. Beringer *et al.* (Particle Data Group), Phys. Rev. D **86** (2012) 010001.
- [2] F. Capozzi *et al.*, arXiv:1312.2878v2.
- [3] M. C. Gonzalez-Garcia *et al.*, *JHEP* **12**, 123 (2012); the updated results obtained after the TAUP2013 International Conference (held in September of 2013) are posted at the URL www.nu-fit.org/?q=node/45.
- [4] A. Aguilar *et al.*, Phys. Rev. D **64** (2001) 112007.
- [5] A.A. Aguilar-Arevalo *et al.*, Phys. Rev. Lett. **105** (2010) 181801.
- [6] A.A. Aguilar-Arevalo *et al.*, Phys. Rev. Lett. **110** (2013) 161801.
- [7] G. Mention *et al.*, Phys. Rev. D **83** (2011) 073006.
- [8] T.A. Mueller *et al.*, Phys. Rev. C **83** (2011) 054615.
- [9] P. Anselmann *et al.*, Phys. Lett. B **342** (1995) 440; W. Hampel *et al.*, Phys. Lett. B **420** (1998) 114.
- [10] J.N. Abdurashitov *et al.*, Phys. Rev. Lett. **77** (1996) 4708, and Phys. Rev. C **59** (1999) 2246.
- [11] B. Armbruster *et al.*, Phys. Rev. D **65** (2002) 112001.
- [12] P. Astier *et al.*, Phys. Lett. B **570** (2003) 19.

- [13] M. Antonello *et al.*, Eur. Phys. J. C **73** (2013) 2345, and Eur. Phys. J. C **73** (2013) 2599.
- [14] N. Agafanova *et al.*, JHEP **1307** (2013) 004 and JHEP **1307** (2013) 085.
- [15] F. Dydak *et al.*, Phys. Lett. B **134** (1984) 281.
- [16] P. Adamson *et al.*, Phys. Rev. Lett. **107** (2011) 011802.
- [17] R. Wendell *et al.*, Phys. Rev. D **81** (2010) 092004.
- [18] P. A. R. Ade *et al.*, arXiv:1303.5076.
- [19] A. Mirizzi *et al.*, arXiv:1303.5368.
- [20] M. Wyman, D. H. Rudd, R. A. Vanderveld and W. Hu, arXiv:1307.7715.
- [21] J. Kopp, P. A. N. Machado, M. Maltoni and T. Schwetz, JHEP **1305** (2013) 050.
- [22] C. Giunti, M. Laveder, Y. F. Li and H. W. Long, Phys. Rev. D **88** (2013) 073008.
- [23] An overview of possible future experiments to test the sterile neutrino hypothesis is given, e.g., in T. Lasserre, talk given at TAUP2013, September 9-13, 2013, Asilomar, California, USA; see also: K. N. Abazajian *et al.*, arXiv:1204.5379.
- [24] A. de Gouvea *et al.*, arXiv:1310.4340.
- [25] M. Yoshimura, Phys. Rev. D **75** (2007) 113007.
- [26] A. Fukumi *et al.*, PTEP **2012** (2012) 04D002.
- [27] D. N. Dinh *et al.*, *Phys. Lett.* **B719** (2013) 154.
- [28] I. Girardi, A. Meroni and S. T. Petcov, JHEP **11** (2013) 146.
- [29] S.M. Bilenky, J. Hosek and S.T. Petcov, Phys. Lett. B **94** (1980) 495.
- [30] M. Archidiacono, N. Fornengo, C. Giunti and A. Melchiorri, Phys. Rev. D **86** (2012) 065028.
- [31] A. A. Aguilar-Arevalo *et al.*, Phys. Rev. Lett. **102** (2009) 101802, and Phys. Rev. Lett. **110** (2013) 161801.
- [32] M. Yoshimura, Phys. Lett. B **699** (2011) 123.
- [33] M. Yoshimura *et al.*, arXiv:805.1970[hep-ph] (2008).
- [34] M. Yoshimura, N. Sasao, and M. Tanaka, Phys. Rev. A **86** (2012) 013812.
- [35] S.T. Petcov, *Phys. Lett.* **B178** (1986) 57.
- [36] NIST (National Institute of Standards and Technology) Atomic Spectra Database: <http://www.nist.gov/pml/data/asd.cfm>
- [37] G. L. Fogli *et al.*, arXiv:1205.5254v3 [hep-ph].